CHEMICAL ENGINEERING TRANSACTIONS
VOL. 63, 2018
A publication of AIDIC
The Italian Association of Chemical Engineering
Online at www.aidic.it/cet
Guest Editors: Jeng Shiun Lim, Wai Shin Ho, Jiří J. Klemeš

ISBN 978-88-95608-61-7; **ISSN** 2283-9216
DOI: 10.3303/CET1863089

Estimation of the Surface Area of a Screen-Printed Carbon Electrode Modified with Gold Nanoparticles and Cysteine using Electrochemical Impedance Spectroscopy

Teh Ubaidah Noh[b], Azila Abd. Aziz[a,b,*]

[a]Institute of Bioproduct Development (IBD), Universiti Teknologi Malaysia, Skudai, Johor
[b]Bioprocess and Polymer Engineering Department, Faculty of Chemical and Energy Engineering, Universiti Teknologi Malaysia, Skudai, Johor
azila@ibd.utm.my

This work concerns with the estimation of the surface area of a screen-printed carbon electrode (SPCE) modified with gold nanoparticles (AuNPs) and cysteine, using electrochemical impedance spectroscopy (EIS). Interpretation of EIS results was based on charge-transfer reactions at high frequencies, followed by diffusion through the monolayers at lower frequencies. Estimates of the electrode fractional surface coverage (θ), active site radius (r_a), and the distance between two adjacent sites ($2r_b$) were obtained by assuming that charge transfer occurred at the active sites and that there were planar diffusions of redox species to these sites. Using EIS, fractional surface coverage was estimated to be around 0.467 for EC modified SPCE, 0.497 for ETSC modified SPCE, and 0.25 for ETSTSC modified SPCE. For the EC modified SPCE, the r_a and $2r_b$ were estimated to be 14.8 µm and 68 µm. For the ETSC modified SPCE, the estimated r_a and $2r_b$ were 14.3 µm and 63.6 µm. The estimated r_a and $2r_b$ for ETSTSC were 13.42 µm and 85 µm. respectively. The inactive site areas for EC, ETSC and ETSTSC modified SPCEs were 0.0587 m^2, 0.0624 m^2, and 0.0314 m^2. The results obtained during this research work suggest that modifying SPCEs using gold and cysteine through electrodeposition of AuNPs, linking with thiourea, self-assembly of AuNPs and self-assembly of cysteine (ETSC) resulted in an electrode with sufficiently high surface area that has the potential to be used as a biosensor for skin sensitiser detection.

1. Introduction

Nowadays, dependency on conventional three electrodes electrochemical cells and bulky electrodes is considered as unfavourable. Instead, quick, small, convenient, low-cost, and disposable electrode systems are desirable. Screen-printed electrode (SPE) addresses the issues of cost viability and portability with simple and inexpensive analytical methods (Hayat and Marty, 2014). One of the most common materials used for deposition on SPE is gold nanoparticles (AuNPs).

Currently, the application of self-assembled monolayer (SAM) technique in the construction of screen-printed carbon electrode (SPCE) has attracted considerable attention since it provides advantages such as ease of preparation, excellent stability, reproducibility, versatility, and the possibility of incorporating different chemical functionalities to produce high molecular order monolayers. AuNPs-SAMs modified techniques are widely used in the fabrication of SPCE since they exhibit excellent selectivity and sensitivity for studies of the electron transfer mechanism (Wong et al., 2011). SAM and different deposition of AuNPs techniques can be combined to produce good reproducibility of modified SPCE. Electrochemical technique such as electrochemical impedance spectroscopy (EIS) can be effectively used to show if the dynamics of charge transfer at the electrochemical interface are strongly controlled by the electrode surface (Kulkarni et al., 2006).

Low molecular weight chemical allergens are referred to as haptens. Haptens are either reactive, electrophilic chemicals, or can be metabolised to reactive metabolites that form covalent bonds with nucleophilic moieties on proteins. There are three main types of nucleophilic moieties present in proteins: thiol (cysteine): hydroxyl (serine, threonine and tyrosine), and amine (lysine and histidine). Covalent modification of skin proteins by

Please cite this article as: Teh Ubaidah Noh, Azila Abd. Aziz, 2018, Estimation of the surface area of a screen-printed carbon electrode modified with gold nanoparticles and cysteine using electrochemical impedance spectroscopy, Chemical Engineering Transactions, 63, 529-534 DOI:10.3303/CET1863089

electrophiles is a key event in the induction of skin sensitisation. In this work, SPCEs were modified with AuNPs and cysteine. Cysteine is an amino acid that has a thiol group, which can bind to AuNPs (Abraham et al., 2010). AuNPs were deposited on the surface of the carbon working electrode, then cysteine was self-assembled on AuNPs, since cysteine cannot be immobilised directly onto a carbon working surface (Wong et al., 2011). EIS analysis was conducted to estimate the surface area of the AuNPs-cysteine modified SPCEs. Characterisation of the AuNPs-cysteine modified SPCE was performed to study the possibility of using the modified SPCE as a biosensor for skin sensitiser detection in a later work.

2. Materials and Methods

2.1 Chemicals Reagents

Potassium ferricyanide 99 % ($K_3Fe(CN)_6$), gold chloride 99.9 % ($HAuCl_4$), cysteine 97 % ($C_3H_7NO_2S$), trisodium citrate dehydrate 98 % ($Na_3C_6H_5O_7$), and potassium chloride 99 % (KCl) were obtained from Sigma-Aldrich, Malaysia. Unless stated otherwise, all chemicals were used as received.

2.2 Electrodes and Equipment

SPCEs (Dropsens), 33 mm length × 10 mm width × 0.5 mm height, were purchased from Metrohm Malaysia Sdn. Bhd. The SPCE consists of three electrodes: carbon working electrode, a carbon auxiliary electrode, and an Ag/AgCl reference electrode. The impedance measurements were determined when the AuNPs-cysteine modified SPCEs were immersed in 10 mL of 1 mM of $K_3Fe(CN)_6$ in 0.1 M KCl as a supporting electrolyte (Viguier et al., 2011).

3. Experimental Procedures

3.1 Modification of SPCE with AuNPs and Cysteine and Estimation of Surface Areas of AuNPs-Cysteine Modified SPCE

Bare SPCEs were washed with 85 % ethanol solution to remove excess dirt on the surface of the carbon-working electrode. SPCEs were modified with AuNPs using three methods. In the first method, 100 µL of $HAuCl_4$ was added to a $Na_3C_6H_5O_7$ solution. The gold (Au) solution was used to electrodeposit AuNPs onto the SPCEs (designated as EC) at +1.1 V for 60 s. In the second method, 6 µL of 0.25 mM thiourea was deposited onto the AuNPs-modified SPCEs (designated as ETSC). Next, Au solution was deposited onto the layer consisting of AuNPs and thiourea – a cross-linker between the two Au layers. In the third method, another layer of thiourea followed by Au solution was added to the whole assembly (designated as ETSTSC). Lastly, 6 µL of 50 mM cysteine was dropped onto the AuNPs-modified SPCEs and left to dry for several minutes in a petri dish under continuous air flow. The summary of the three methods is shown in Figure 1. EIS analysis was conducted and the experiment data were measured when the AuNPs-cysteine modified SPCEs were immersed in 1 mM of $K_3Fe(CN)_6$ in 0.1 M KCl.

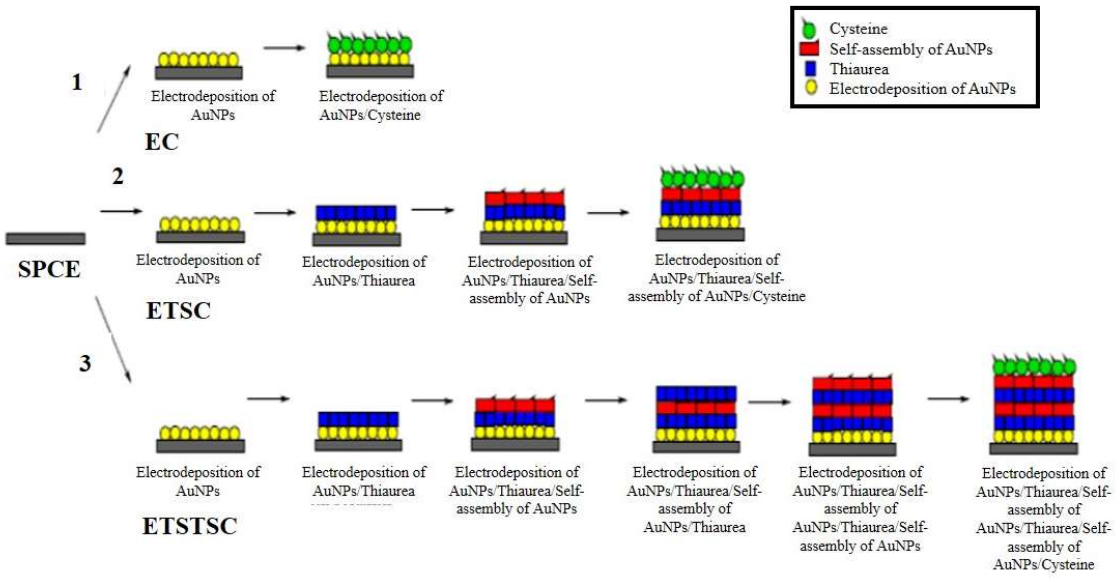

Figure 1: Summary of the modifications of SPCEs

Surface areas of the modified electrodes were estimated by comparing the θ, r_a, and r_b values for the EC, ETSC and ETSTSC modified SPCE. Randles circuit could be used to describe the total impedance of the system. The total impedance may be described by Eq(1).

$$Z = Rs + \frac{R_{CT} + Z_D}{1 + \sigma\omega^{1/2}C_{dl} + j(R_{CT}\omega C_{dl} + \sigma\omega^{1/2}C_{dl})} \quad (1)$$

where,

$$R_{CT} = \frac{RT}{nFI_0} \quad (2)$$

$$Z_D = \sigma\omega^{-1/2}(1- j) \quad (3)$$

R, T, n, and F have their usual meanings, and i_0 is the current exchange density, which is directly related to the rate constant for the charge transfer reaction. Eq(4) is used to calculate the Warburg coefficient, σ, assuming equal concentrations, C, and diffusion coefficients, D, for both oxidised and reduced species.

$$\sigma = \frac{\sqrt{2RT}}{n^2F^2CA\sqrt{D}} \quad (4)$$

Matsuda et al. (1979) and Finklea et al. (1993) derived equations for the impedance of electrodes having θ values lower and greater than 0.9, assuming equal concentrations and diffusion coefficients of the oxidised and reduced species. For θ > 0.9, the equations for the electrode impedance were derived from microarray electrodes, based on the nonlinear diffusion at these types of the electrode described by Ferreira et al. (2009). According to Finklea et al. (1993), the equations for the real Faradaic impedance are similar for both situations, except for the value of the parameter q, which described the relationship between the diffusion coefficient and the microelectrode dimensions. For (1-θ) > 0.1 and (1-θ) < 0.1, Eq(5) that described the real Faradaic impedance is given as:

$$Z'_f = \frac{R_{CT}}{1-\theta} + \frac{\sigma}{\sqrt{\omega}} + \frac{\sigma}{1-\theta}\left\{\frac{[(\omega^2+q^2)^{1/2}+q]}{(\omega^2+q^2}\right\}^{1/2} \quad (5)$$

where, R_{CT}, σ, and ω, and q is given by Eq(5) or Eq(6) (Ferreira et al., 2009)

$$q = \frac{2D}{[r_b^2\theta(1-\theta)\ln(1+0.27/(1-\theta)^{1/2}]} \qquad \text{for} \quad (1-\theta) > 0.1 \quad (6)$$

The Faradaic impedance for high frequencies is described by Eq(7) (Janek et al., 1998):

$$Z'_f = \frac{R_{CT}}{1-\theta} + m\omega^{-1/2} \quad (7)$$

where,

$$m = \sigma + \frac{\sigma}{1-\theta} \quad (8)$$

4. Results and Discussion

4.1 Estimation of Surface Areas and Fractional Surface Coverage (θ) of AuNPs-Cysteine Modified SPCE

The surface area of AuNps-cysteine modified SPCE can be calculated using CV and EIS. The values of θ_{CV}^{P} are qualitatively similar to the trend in θ_{IS}^{R} , but the size of θ_{CV}^{P} is always less than θ_{IS}^{R} . The resulting estimation of surface area by different scan rate using CV is also considered as invalid since the calculated surface areas are illogical for SPCE. The electrochemical impedance technique was used for the surface fractional coverage estimations. The variance in the estimation of θ is explained better if the radial diffusion to the micropores in the SAM film is influenced. According to Finklea et al. (1993), if radial diffusion to micropores occurred, then the peak current observed is not a simple function of the exposed area of the SAM modified SPCE. The distribution and radial size of the pores was considered to adequately describe the surface structure and the effects on electron transfer.

The experimental impedance data for the modified SPCE were well described by the Randles circuit. Table 1 and Figure 2 shows the parameters that best fitted the experimental data.

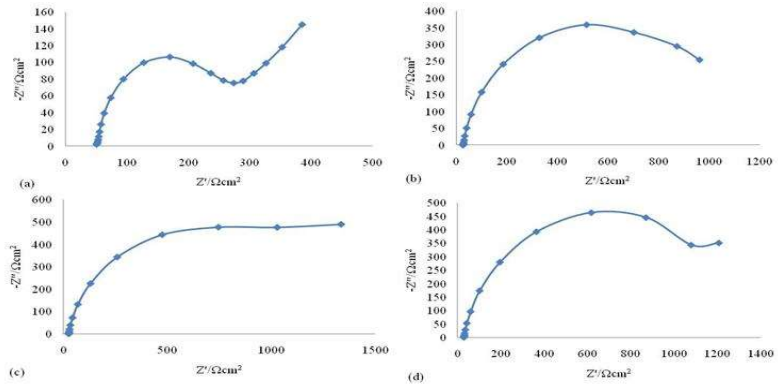

Figure 2: Nyquist plots of different modified SPCEs in 1 mM $Fe(CN)_6^{3-/4-}$ containing 0.1 M KCl at 10 mV/s (a) AuNPs, (b) EC, (c) ETSC and (d) ETSTSC

The experimental and simulated imaginary (-Z") vs. real (Z') impedance plots (Figure 2) for the modified SPCEs in 1 mM of $Fe(CN)_6^{3-/4-}$ containing 0.1 M KCl. All the (–Z") vs. (Z') complex plane plots show a semicircle at high frequencies, which can be related to the interfacial capacitance in parallel to the effective charge-transfer resistance, $R_{CT}/(1-\theta)$, where $(1-\theta)$ represents the active area of the electrode for the $Fe(CN)_6^{3-/4-}$ redox couple. This semicircle is followed by another capacitive loop showing linear behaviour. The slope of the straight line is not unity, suggesting irregular diffusion behaviour (Ferreira et al. 2009). The effect of mass transport could be represented by diffusion impedance, Z_D. The equivalent circuit was closely fitted the experimental impedance data for modified electrodes, but the mass transfer impedance was not pure as Warburg impedance. Z_D is represented by CPE2 for EC, ETSC and ETSTSC modified SPCE. The results of the fitting of the experimental data are given in Table 1.

Table 1: The data that fit the experimental impedance data

Type of modified layer of SPCE	Rs (Ω cm^2)	CPE1 (μS cm^2 S$^{\alpha-1}$)	α_1	$R_{ct.app}$[a] (Ω cm^2)	CPE2 (μS cm^2 S$^{\alpha-1}$)	α_2	R_d (Ω cm^2)
AuNPs layer	47.56	23.71	0.82	258.31	2.46	0.75	-
EC	56.65	1.39	0.90	1515.49	5.88	0.80	3.78
ETSC	25.47	11.89	0.99	1864.66	11.89	0.63	3.07
ETSTSC	31.20	580.56	0.99	884.12	27.82	0.81	27.01

$R_{ct.app}$[a] = $R_{ct}/(1 - \theta)$; capacitance = CPE $(\omega_{max})^{\alpha-1}$

A model based on the work of Matsuda et al. (1979) and Amatore et al. (1983) was developed to fit the Faradaic impedance data for charge transfer reactions at the perforated SAM-coated electrodes to understand the nature of the pores in SAMs. The use of CPE with α deviated from 0.5, connected in parallel to a diffusion resistance, R_d, described the diffusion impedance and represented the finiteness of the length of the diffusion path. In some cases, the error in R_d was high; suggesting that the corresponding time constant was due to a diffusion response rather than a resistive one. Rs and (R_{CT}CPE1) have the same meaning. The sub-circuit (R_dCPE2) represented the mass transport perturbed by the protein-SAM layer on the modified SPCE as shown in Figure 3.

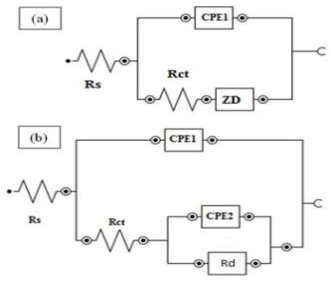

Figure 3 : Equivalent ideal Randles circuit

For the ETSC modified SPCE, linear diffusion characteristic almost disappeared as the apparent R_{CT} increased, due to blockage of the electrode surface (Figure 2c). This might be because the diffusion process

was in the same frequency region as the R_{CT} and this occurrence dominated the total impedance response.
For EC and ETSTSC modified SPCEs, the R_{CT} values were somewhat lower, and the capacitance were higher, than that of the bare electrode. When the cysteine and AuNPs were immobilised on SAMs, the apparent charge transfer resistance increased, and the capacitance decreased. The increase in R_{CT} value indicated a partially blocked surface, which inhibited the electron transfer process since access of the redox species to the SPCE was impeded. The positive charge on EC and ETSTSC modified SPCEs can be partially or entirely compensated by the presence of the protein diminishing the capacitance. The increase in the layer thickness, following protein immobilisation, also reduced the capacitance. The α_1 values were around 0.9, suggesting that the current distribution on the electrode surface was similar to that of an ideal capacitor.
The estimates of the size of active and inactive sites, surface coverage, or the diffusion coefficients of the redox couple species can be obtained when the following are considered: (1) $\alpha_1 \geq 0.9$, so that a capacitor could replace CPE1; (2) a linear behaviour of complex plane plots is observed at the beginning of the second capacitive loop, suggesting a mass transport control at the low-frequency region; (3) the AuNPs-cysteine modified SPCE can be considered to form active sites with radius of r_a, where the oxidation and reduction electron-transfer reactions of a redox couple may occur. The active sites represent the unmodified surface, with a total area equal to A(1- θ), where A is the area of the working surface of SPCE; the distances between two adjacent active sites are $2r_b$, where r_b is the radius of the inactive domain surrounding the pinhole; (4) the active sites are surrounded by an inactive region, and the total inactive area is Aθ; (5) the diffusion of redox species to the AuNPs areas of the SPCE is planar, and as a first approximation this diffusion can be considered as semi-infinite.
When ω = 0, R_{CT} and σ can be estimated from the intercept and the slope of the Faradaic impedance plot, (Z'_f) vs. $(\omega^{-1/2})$. The Faradaic impedance (Z'_f) can be obtained by subtracting the solution resistance (Rs) from the real impedance values (Ferreira et al. 2009). In this experiment, Rs value was around 47.56 Ωcm^2. Based on the equation of the real Faradaic impedance plot, (Z'_f) vs. $(\omega^{-1/2})$. (Figure 4), the y-intercept gave the R_{CT} value ~ca. 258.31 $\Omega\ cm^2$, and the slope of the linear section in the low-frequency region gave a σ value of 25 $cm^2\ rad^{1/2}\ s^{1/2}$. From Eq(8), a redox species diffusion coefficient of $D = 1.21 \times 10^{-8}\ cm^2\ s^{-1}$ was obtained.

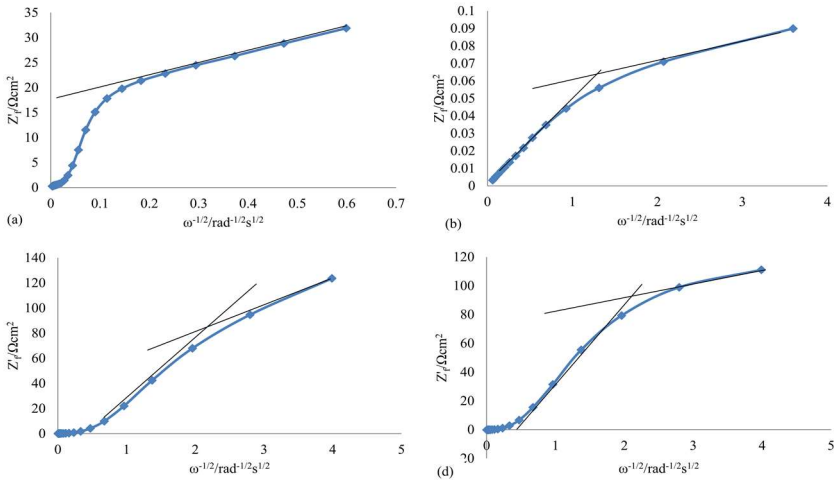

Figure 4: Faradaic impedance plots, (Z'_f) vs. $(\omega^{-1/2})$, in the presence of 1 mM of $Fe(CN)_6^{3-/4-}$ containing 0.1 M KCl: (a) AuNPs SPCE; (b) EC; (c) ETSC; and (d) ETSTSC; A = 0.13 cm^2

The relationship between r_a, r_b and θ can be derived on a geometrical basis as $(1 - \theta) = r_a^2/r_b^2$. All parameters related to the active and inactive sites can be estimated using Eq(6) for $(1 - \theta) < 0.1$, since precise Rs corrections can be made.
Considering that a precise Rs correction may be easily achieved, all the parameters of interest can be estimated from an analysis of the high and low-frequency regions of the real Faradaic impedance plots, (Z'_f) vs. $(\omega^{-1/2})$. For such evaluation, the q value can also be estimated from (Z'_f) vs. $(\omega^{-1/2})$ plots. Figure 4 shows the (Z'_f) vs. $(\omega^{-1/2})$ plots for the $Fe(CN)_6^{3-/4-}$ redox couple on AuNPs-cysteine modified SPCE. According to Matsuda et al. (1979), the q value can be obtained from the intersection of the lines at high and low-frequency domains of (Z'_f) as = q/2, and the nearest spacing between pinholes can be estimated from Eq(6). For the ETSC modified SPCE, a value of $m = 49.74\ \Omega\ cm^2\ rad^{1/2}\ s^{-1/2}$ was obtained from the slope of the (Z'_f) vs. $(\omega^{-1/2})$ plot in the high-frequency region (Figure 4c). Considering $\sigma = 25\ cm^2\ rad^{1/2}\ s^{-1/2}$, which was obtained from the

AuNPs modified SPCE (Figure 4a), θ = 0.497 was found from Eq(13). The intersection between high and low-frequency domains resulted in a value of q= 164. Using Eq(6), with D = 1.21×10^{-8} cm^2 s^{-1} and (1-θ)= r_a^2/r_b^2, the radius r_a and r_b were calculated as 14.3 μm and 31.8 μm.

Using the same procedure, the θ values for both EC modified SPCE (Figure 4b) and ETSTSC modified SPCE (Figure 4d) were estimated to be 0.467 and 0.25. Since the estimated θ value was lower than 0.9, r_a and r_b values were estimated using Eq(8). The q values for both EC modified SPCE and ETSTSC modified SPCE, obtained from the intersection between the high and low-frequency domains were 152 and 186. For EC modified SPCE, the values of r_a and r_b were 14.8 μm and 34 μm; while ETSTSC modified SPCE, the values of r_a and r_b were 13.42 μm and 42.5 μm. The inactive site area for EC, ETSC and ETSTSC modified layer were 0.0587 m^2, 0.0624 m^2, and 0.0314 m^2 and the active site area for EC, ETSC, and ETSTSC modified layer were 0.0669 m^2, 0.0632 m^2, and 0.0942 m^2. Lastly, the values of $2r_b$ for EC, ETSC and ETSTSC modified SPCE were 68 μm, 63.6 μm, and 85 μm.

These values were considered as estimations based on the initial assumptions made prior to the calculation. For example, typical Warburg behaviour was assumed, but the experimental data indicated some deviation from such behaviour. This implies the possibility of a non-uniform spatial distribution of pinholes, with the formation of patches in which the diffusion layers could not overlap, and so on.

5. Conclusion

The estimates of the surface area of EC, ETSC, and ETSTSC modified SPCEs have been obtained using EIS. Using EIS, surface coverage was estimated to be around 0.467 for EC modified SPCE, 0.497 for ETSC modified SPCE, and 0.25 for ETSTSC modified SPCE. For EC, ETSC, ETSTSC modified SPCE, the r_a were estimated to be 14.8 μm, 14.3 μm and 13.42 μm. The inactive site areas for EC, ETSC and ETSTSC modified SPCEs were 0.0587 m^2, 0.0624 m^2, and 0.0314 m^2 respectively. Lastly, the $2r_b$ for EC, ETSC, and ETSTSC modified SPCEs was 68 μm, 63.6 μm and 85 μm. The results obtained during this research work suggest that modifying SPCEs using AuNPs and cysteine through electrodeposition of AuNPs, linking with thiourea, self-assembly of AuNPs and self-assembly of cysteine (ETSC) resulted in an electrode with sufficiently high surface area that has the potential to be used as a biosensor for skin sensitiser detection.

Acknowledgments

The authors would like to thank Universiti Teknologi Malaysia (Vot: Q.J130000.2546.14H71) and Ministry of Higher Education (MyBrain scholarship) for financial supports.

References

Abraham A., Mihaliuk E., Kumar B., Legleiter J., Gullion T., 2010, Solid-state NMR study of cysteine on gold nanoparticles, The Journal of Physical Chemistry C, 114 (42), 18109-18114.

Amatore C., Saveant J. M., Tessier D., 1983, Charge transfer at partially blocked surfaces: A model for the case of microscopic active and inactive sites, Journal of Electroanalytical Chemical, 147, 39-51.

Ferreira A.A.P., Fugivara C.S., Barrozo S., Suegama P.H., Yamanaka H., Benedetti A.V., 2009, Electrochemical and spectroscopic characterization of screen-printed gold-based electrodes modified with self-assembled monolayers and Tc85 protein, Journal of Electroanalytical Chemistry, 634 (2), 111-122.

Finklea H.O., Sinder D.A., Fedyk J., Sabatini E., Gaini Y., Rubinstein I., 1993, Characterization of octadecanethiol-coated gold electrodes as microarray electrodes by cyclic voltammetry and ac impedance spectroscopy, Langmuir, 9, 3660.

Hayat A., Marty J. L., 2014, Disposable screen printed electrochemical sensors: Tools for environmental monitoring, Sensors (Switzerland), 14 (6), 10432-10453.

Janek R.P., Fawcett W.R., Ulman A., 1998, Impedance spectroscopy of self-assembled monolayers on Au(111): Sodium ferrocyanide charge transfer at modified electrodes, Langmuir, 14, 3011-3018.

Kulkarni S.A., Mulla I.S., Vijayamohanan K., 2006, Electrochemical characterization of self-assembled monolayers on semiconducting substrates for MEMS applications, Journal of Physics: Conference Series, 34, 322-329.

Matsuda H., Tokuda K., Gueshi T., 1979, Voltammetry at partially covered electrodes: Part III. Faradaic impedance measurements at model electrodes, Journal of Electroanalytical Chemistry, 102, 41-48.

Wong P.S., Nathan S., Yook Heng L., 2011, A disposable copper (II) ion biosensor based on self-assembly of L-cysteine on gold nanoparticle-modified screen-printed carbon electrode, Journal of Sensors, 2011, 1-15.

Viguier B., Zor K., Kasotakis E., Mitraki A., Clausen C.H., Svendsen W.E., Castillo-Leon J., 2011, Development of an electrochemical meta-ion biosensor using self-assembled peptide nanofibrils, ACS Applied Materials & Interfaces, 3 (5), 1594-1600.